

Proceedings Article

# Dual mode imaging of phantoms in two orthogonal planes with a single-sided FFL MPI scanner

Chris McDonough <sup>a</sup> · John Chrisekos <sup>a</sup> · Alexey Tonyushkin <sup>a,\*</sup>

<sup>a</sup>Physics Department, Oakland University, Rochester, MI 48309 USA

\*Corresponding author, email: [tonyushkin@oakland.edu](mailto:tonyushkin@oakland.edu)

© 2024 McDonough *et al.*; licensee Infinite Science Publishing GmbH

This is an Open Access article distributed under the terms of the Creative Commons Attribution License (<http://creativecommons.org/licenses/by/4.0>), which permits unrestricted use, distribution, and reproduction in any medium, provided the original work is properly cited.

## Abstract

A number of MPI scanner configurations have recently emerged in pursuit of clinical imaging capabilities. A single-sided scanner stands out as one of the promising designs, featuring hardware located exclusively on one side of the device. This approach grants the scanner access to an unhindered imaging volume. Our research group has suggested and developed a variant of the single-sided scanner employing Field-Free Line (FFL) for spatial encoding. In this work, we present the complete small-scale prototype of an FFL MPI scanner by demonstrating imaging phantoms in two orthogonal planes using two different imaging methods.

## I. Introduction

Magnetic Particle Imaging (MPI) is an emerging medical imaging modality with great potential for diagnostics and biopsy of cancer [1] and interventional procedures [2]. Conventional MPI scanners employ a closed bore topology [3] or narrow opening [4], that may result in high cost and complexity of scaling this design to achieve whole-body imaging. As a result, there is a need for a specialized body-part or specific application scanner that can efficiently provide a clinically viable solution. In this regard the single-sided scanner topology [5], which consolidates all hardware components on a single side of the device, could serve the clinical needs for local exams.

Compared to the other available single-sided scanner that relies on a field-free point (FFP) approach [6, 7] our design [8, 9] harnesses the potential of a field-free line (FFL) [10] that has several advantages, including higher sensitivity [11] and access to robust reconstruction techniques [12]. Previous research has showcased the device's capability to perform 1D imaging [13] and initial 2D imag-

ing [14] achieved through manual rotation of rod phantoms. This study, presents a significant advancement by demonstrating experimental imaging of phantoms in two orthogonal planes utilizing different imaging techniques. The new capabilities are made possible by the integration of a custom-designed electronic rotation table, which facilitates automatic subject rotation and allows for height adjustments during imaging thus demonstrating the proof of principal of our MPI scanner.

## II. Methods and materials

### II.1. Single-Sided Scanner

The coil system of our FFL single-sided scanner is described in details in [9]. The setup consists of a water cooled enclosure with three elongated electromagnetic coils. Two of the embedded coils are responsible for creating the FFL and used for spatial encoding. Applying variable DC currents to these selection coils creates the FFL above the surface of the scanner and moves it across

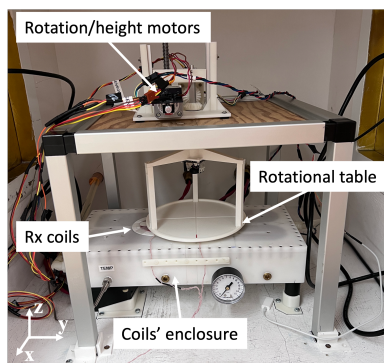


**Figure 1:** Single-sided FFL scanner setup with a rotational subject's table.

the short axis of our scanner. The third embedded coil located below the selection coils in the center of the scanner is used for the excitation of the superparamagnetic iron oxide (SPIO) sample. In addition to the enclosed coils there are two circular coils located at the surface of the scanner that are used as the receive coils in a surface gradiometer arrangement [11].

To implement tomographic imaging we designed and built a custom electronic rotation subject table with the electronic height adjustment as shown in Fig. 1. The subject table is capable of automatic rotation of the subject with a maximum angular resolution of  $1.8^\circ$ , and of height adjustment with a step size of  $1/100$  mm. Rotation and height are controlled by two separate stepper motors, allowing for simultaneous adjustment of the subject in both angle and vertical positions.

## II.II. Phantoms

To demonstrate the scanner's imaging capability in the horizontal  $xy$  plane, we used an "OU" phantom (see Fig. 2 (a,c)), with each letter filled with undiluted Synomag-D SPIO. For 2D projection imaging in the vertical  $xz$  plane, we employed phantoms consisting of glass rods measuring 30 mm in length and 1 mm in diameter, filled with undiluted Synomag-D SPIO. These rods were oriented in the horizontal plane and inserted into holes of a 3D printed holder, ensuring their placement at different positions and heights in the  $xz$  plane (see Fig. 3).

## II.III. Imaging

For imaging in the horizontal  $xy$  plane, the letter phantoms were positioned on a rotating subject table capable of automatic rotation from  $0^\circ$  to  $180^\circ$ , providing a total field of view (FOV) of  $4\text{ cm} \times 4\text{ cm}$  at a fixed height. The FFL was scanned across the  $x$  direction of the phantom with a step size of 1 mm, ranging from  $-2\text{ cm}$  to  $2\text{ cm}$ , to capture a projection and the background signal was subtracted from the average. Subsequently, the subject

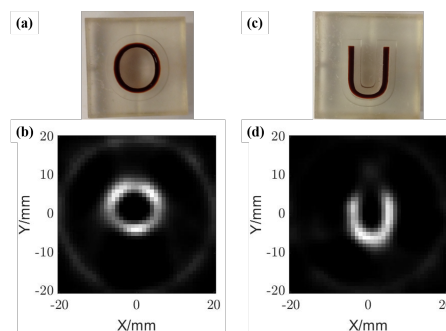


**Figure 2:** a), c) 3D printed "O" and "U" phantoms and b), d) the corresponding experimentally obtained images in the horizontal plane.

table was rotated, and the process was repeated to obtain projections at various angles. This procedure was conducted for 20 angles spanning from  $0^\circ$  to  $180^\circ$ . Each projection takes 8 s to complete and the total imaging time for the horizontal plane image is 10 min. It has been optimized for maximum background reduction rather than speed. All stepper motors are switched off during signal acquisition step to remove any interference.

The recorded projections were processed using filtered-backprojection (FBP) image reconstruction and were deconvolved using a simulated point spread function. This reconstruction technique and imaging mode, in general, required a homogeneous magnetic field gradient, meaning all positions of the FFL must have a similar magnetic field gradient. Consequently, the magnitude of the gradient magnetic field in the center of the FOV was limited to  $0.58\text{ T/m}$ .

For imaging in the vertical plane the FFL is scanned across subject in  $xz$  plane to obtain a 2D projection image. The FFL trajectory is following an arc along  $x$  direction, and then the subject is mechanically raised in the  $z$  direction by the automatic height adjustment of  $0.5\text{ mm}$  in order to image the phantom at different heights. Imaging in this mode allows us to use an inhomogeneous magnetic field gradient, which varies with the position of the FFL so that the magnetic field gradient is maximum at the center of the FOV with a magnitude of  $0.84\text{ T/m}$ .

## III. Results and Discussion

The experimental results of imaging "O" and "U" phantoms in the horizontal plane are shown in Fig. 2 (b,d). Here, we utilized the conventional FBP technique for image reconstruction [12]. However, due to field inhomogeneity the effective imaging volume is currently limited by  $2\text{ cm} \times 2\text{ cm}$ .

The experimental study of imaging in the vertical plane is presented in Fig. 3, where 2D projection images of rods appear as dots in  $xz$  plane. In this study we varied the number of rods and their respective position along

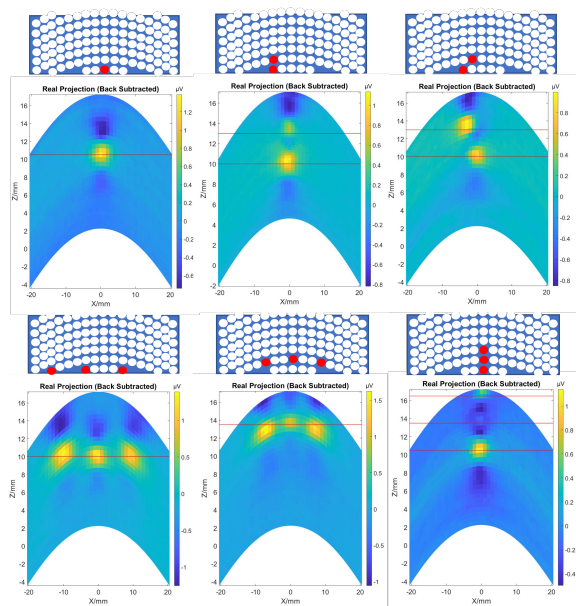


**Figure 3:** Experimental images in the vertical plane of a single, double, and triple rod phantoms and the corresponding rod positions in a 3D printed holder. Here the red lines show the z coordinate of the rods with respect to the surface of the scanner.

the horizontal and the vertical axes as shown on the top schematic picture of each respective image. The top row images show a single and two rods shifted vertically by 3 mm and horizontally by 2.5 mm, where the crossed red lines indicate the height of the rods. The bottom row images show three rods arranged horizontally in two different heights or vertically. The smallest separation between the two adjacent rods is 7.5 mm. The results of the imaging in the vertical plane demonstrate the FOV of 0.6 mm along z axis and spatial resolutions of 3 mm and 7.5 mm, in the z and x directions, respectively. By employing this imaging method we demonstrated an alternative technique using the FFL to project phantoms into a 2D plane at fixed angular position. Obtaining such projections at multiple angles would in principle allow to implement 3D FBP imaging of a subject. Imaging of a subject through different heights, however, results in negative lobe artifacts, which manifest themselves as dark spots and may result in negative interference. We plan to address the artifacts in future studies by updating the reconstruction technique.

## IV. Conclusion

In this work we presented imaging in two orthogonal planes of phantoms with our single-sided FFL MPI scanner. We have demonstrated FBP imaging in the horizontal plane and 2D projection imaging in the vertical plane by imaging "OU" and rods phantoms. We demonstrated the spatial resolution of 3 mm and 7.5 mm in the z and

x directions, respectively. This results provide proof of principle for our single-sided FFL MPI scanner.

## Acknowledgments

Research funding: this work is supported by NIH under Award R15EB028535.

## Author's statement

Conflict of interest: Authors state no conflict of interest.

## References

- [1] E. E. Mason, E. Mattingly, K. Herb, M. Śliwiak, S. Franconi, C. Z. Cooley, P. J. Slanetz, and L. L. Wald. Concept for using magnetic particle imaging for intraoperative margin analysis in breast-conserving surgery. *Scientific Reports*, 11(1):13456, 2021, doi:[10.1038/s41598-021-92644-8](https://doi.org/10.1038/s41598-021-92644-8).
- [2] P. Vogel, M. A. Rückert, C. Greiner, J. Günther, T. Reichl, T. Kampf, T. A. Bley, V. C. Behr, and S. Herz. Impi: Portable human-sized magnetic particle imaging scanner for real-time endovascular interventions. *Scientific Reports*, 13:10472, 1 2023, doi:[10.1038/s41598-023-37351-2](https://doi.org/10.1038/s41598-023-37351-2).
- [3] B. Gleich and J. Weizenecker. Tomographic imaging using the nonlinear response of magnetic particles. *Nature*, 435(7046):1214–1217, 2005, doi:[10.1038/nature03808](https://doi.org/10.1038/nature03808).
- [4] C. B. Top and A. Güngör. Tomographic field free line magnetic particle imaging with an open-sided scanner configuration. *IEEE Transactions on Medical Imaging*, 39(12):4164–4173, 2020, doi:[10.1109/TMI.2020.3014197](https://doi.org/10.1109/TMI.2020.3014197).
- [5] T. F. Sattel, T. Knopp, S. Biederer, B. Gleich, J. Weizenecker, J. Borgert, and T. M. Buzug. Single-sided device for magnetic particle imaging. *Journal of Physics D: Applied Physics*, 42(2):022001, 2009, doi:[10.1088/0022-3727/42/2/022001](https://doi.org/10.1088/0022-3727/42/2/022001).
- [6] K. Gräfe, A. von Gladiss, G. Bringout, M. Ahlborg, and T. M. Buzug. 2D Images Recorded With a Single-Sided Magnetic Particle Imaging Scanner. *IEEE Transactions on Medical Imaging*, 35(4):1056–1065, 2016, doi:[10.1109/TMI.2015.2507187](https://doi.org/10.1109/TMI.2015.2507187).
- [7] A. von Gladiss, Y. Blancke Soares, T. M. Buzug, and K. Gräfe. Dynamic imaging with a 3d single-sided mpi scanner, in *International Workshop on Magnetic Particle Imaging*, 235–236, 2019.
- [8] A. Tonyushkin. Single-Sided Field-Free Line Generator Magnet for Multi-Dimensional Magnetic Particle Imaging. *IEEE Transactions on Magnetics*, 53(9):5300506, 2017, doi:[10.1109/TMAG.2017.2718485](https://doi.org/10.1109/TMAG.2017.2718485).
- [9] J. Pagan, C. McDonough, T. Vo, and A. Tonyushkin. Single-sided magnetic particle imaging device with field-free-line geometry for in vivo imaging applications. *IEEE Transactions on Magnetics*, 57(2):5300105, 2021, doi:[10.1109/TMAG.2020.3008596](https://doi.org/10.1109/TMAG.2020.3008596).
- [10] J. Weizenecker, B. Gleich, and J. Borgert. Magnetic particle imaging using a field free line. *Journal of Physics D: Applied Physics*, 41(10):105009, 2008, doi:[10.1088/0022-3727/41/10/105009](https://doi.org/10.1088/0022-3727/41/10/105009).
- [11] C. McDonough, J. Pagan, and A. Tonyushkin. Implementation of the surface gradiometer receive coils for the improved detection limit and sensitivity in the single-sided mpi scanner. *Physics in Medicine & Biology*, 67(24):245009, 2022, doi:[10.1088/1361-6560/aca5ec](https://doi.org/10.1088/1361-6560/aca5ec).
- [12] C. Chinchilla, C. McDonough, A. Negash, J. Pagan, and A. Tonyushkin. Simulation studies of image reconstruction for field free line single-sided magnetic particle imaging scanner. *International journal on magnetic particle imaging*, 7(1):2104001, 2021.

- [13] C. McDonough, D. Newey, and A. Tonyushkin. 1-d imaging of a superparamagnetic iron oxide nanoparticle distribution by a single-sided ffl magnetic particle imaging scanner. *IEEE Transactions on Magnetics*, 58(8):6501105, 2022, doi:[10.1109/TMAG.2022.3151710](https://doi.org/10.1109/TMAG.2022.3151710).
- [14] C. McDonough and A. Tonyushkin. 2d projection imaging with a single-sided ffl magnetic particle imaging scanner. *International journal on magnetic particle imaging*, 9(1):Suppl 1, 2023, doi:[10.18416/IJMPI.2023.2303028](https://doi.org/10.18416/IJMPI.2023.2303028).